



University of Groningen

Observation of large refrigerant capacity in the HoVO₃ vanadate single crystal

Balli, M.; Roberge, B.; Jandl, S.; Fournier, P.; Palstra, T. T. M.; Nugroho, A. A.

Published in:
Journal of Applied Physics

DOI:
[10.1063/1.4929370](https://doi.org/10.1063/1.4929370)

IMPORTANT NOTE: You are advised to consult the publisher's version (publisher's PDF) if you wish to cite from it. Please check the document version below.

Document Version
Publisher's PDF, also known as Version of record

Publication date:
2015

[Link to publication in University of Groningen/UMCG research database](#)

Citation for published version (APA):

Balli, M., Roberge, B., Jandl, S., Fournier, P., Palstra, T. T. M., & Nugroho, A. A. (2015). Observation of large refrigerant capacity in the HoVO₃ vanadate single crystal. *Journal of Applied Physics*, 118(7), 073903-1 - 073903-5. [073903]. <https://doi.org/10.1063/1.4929370>

Copyright

Other than for strictly personal use, it is not permitted to download or to forward/distribute the text or part of it without the consent of the author(s) and/or copyright holder(s), unless the work is under an open content license (like Creative Commons).

Take-down policy

If you believe that this document breaches copyright please contact us providing details, and we will remove access to the work immediately and investigate your claim.

Downloaded from the University of Groningen/UMCG research database (Pure): <http://www.rug.nl/research/portal>. For technical reasons the number of authors shown on this cover page is limited to 10 maximum.

Observation of large refrigerant capacity in the HoVO_3 vanadate single crystal

M. Balli, B. Roberge, S. Jandl, P. Fournier, T. T. M. Palstra, and A. A. Nugroho

Citation: [Journal of Applied Physics](#) **118**, 073903 (2015); doi: 10.1063/1.4929370

View online: <https://doi.org/10.1063/1.4929370>

View Table of Contents: <http://aip.scitation.org/toc/jap/118/7>

Published by the [American Institute of Physics](#)

Articles you may be interested in

[Advanced materials for magnetic cooling: Fundamentals and practical aspects](#)
[Applied Physics Reviews](#) **4**, 021305 (2017); 10.1063/1.4983612

[Analysis of the phase transition and magneto-thermal properties in \$\text{La}_2\text{CoMnO}_6\$ single crystals](#)
[Journal of Applied Physics](#) **116**, 073907 (2014); 10.1063/1.4893721

[Giant magnetocaloric effect and temperature induced magnetization jump in \$\text{GdCrO}_3\$ single crystal](#)
[Journal of Applied Physics](#) **117**, 133901 (2015); 10.1063/1.4916701

[Mechanical properties and magnetocaloric effects in \$\text{La}\(\text{Fe}, \text{Si}\)_{13}\$ hydrides bonded with different epoxy resins](#)
[Journal of Applied Physics](#) **117**, 063902 (2015); 10.1063/1.4908018

[Observation of the large magnetocaloric effect and suppression of orbital entropy change in Fe-doped \$\text{MnV}_2\text{O}_4\$](#)
[Journal of Applied Physics](#) **115**, 034903 (2014); 10.1063/1.4861630

[A study of the phase transition and magnetocaloric effect in multiferroic \$\text{La}_2\text{MnNiO}_6\$ single crystals](#)
[Journal of Applied Physics](#) **115**, 173904 (2014); 10.1063/1.4874943

AIP | Journal of
Applied Physics

SPECIAL TOPICS



Observation of large refrigerant capacity in the HoVO_3 vanadate single crystal

M. Balli,^{1,a)} B. Roberge,¹ S. Jandl,¹ P. Fournier,^{1,2} T. T. M. Palstra,³ and A. A. Nugroho⁴

¹*Regroupement québécois sur les matériaux de pointe, Département de physique, Université de Sherbrooke, Quebec J1K 2R1, Canada*

²*Canadian Institute for Advanced Research, Toronto, Ontario M5G 1Z8, Canada*

³*Solid State Chemistry Laboratory, Zernike Institute for Advanced Materials, University of Groningen, Nijenborgh 4, 9747 AG Groningen, The Netherlands*

⁴*Department of Physics, Faculty of Mathematics and Natural Sciences, Institut Teknologi Bandung, 40132 Bandung, Indonesia*

(Received 6 July 2015; accepted 11 August 2015; published online 21 August 2015)

The HoVO_3 orthovanadate undergoes a large negative and conventional magnetocaloric effects around 4 K and 15 K, respectively. The partly overlapping of the magnetic transition at 15 K and the structural transition occurring at 40 K, as well as the large magnetization, give rise to a giant refrigerant capacity without hysteresis loss. For a magnetic field variation of 7 T, the refrigerant capacity is evaluated to be 620 J/kg, which is larger than that for any known RMnO_3 manganite. These results should inspire and open new ways for the improvement of magnetocaloric properties of ABO_3 type-oxides. © 2015 AIP Publishing LLC. [<http://dx.doi.org/10.1063/1.4929370>]

I. INTRODUCTION

The magnetic refrigeration based on the magnetocaloric effect (MCE) exhibited by many magnetic substances emerges as a promising alternative for conventional systems due to its higher energy saving and eco-friendly nature.^{1–7} Magnetocaloric refrigeration can be implemented in a wide temperature range covering household and industrial applications, gas liquefaction, academic research, and space industry. The manganite perovskite oxides are amongst the most promising magnetocaloric refrigerants,^{8–11} particularly for application at low temperature regime because of their large corrosion resistance, high electric resistance (which minimizes the energy loss), low hysteresis, and mechanical stability.⁸ On the other hand, the ABO_3 -type transition-metal oxides (A = rare earth) have attracted considerable attention during the last two decades because of their fascinating physical properties such as colossal magneto-resistance, high-temperature superconductivity, and magnetocaloric effect. Several manganites of formula RMnO_3 (R = rare earth) exhibit a strong interplay between their magnetic and electric degrees of freedom, opening the way for their incorporation into practical spintronic devices.^{12,13} Additionally, several studies of the RMnO_3 magnetocaloric properties have been carried out, finding a high potential use for magnetic cooling.^{8,11} For low temperature applications, numerous materials such as $(\text{Ho}, \text{Tb}, \text{Dy})\text{MnO}_3$ have been proposed.^{10,14,15} In contrast, the magnetocaloric potential of the RVO_3 vanadates has not yet been explored. However, perovskite-type vanadium oxides RVO_3 provide a variety of phase transitions associated with the nearly degenerate vanadium t_{2g} orbitals, which could impact favourably the magnetocaloric performance.

The RVO_3 perovskite orthovanadates^{16–18} usually exhibit an orthorhombic crystal structure with Pbnm space group at

room temperature. Up to now, in the HoVO_3 system, mainly three magnetic transitions were reported in the literature.^{16–18} At ~ 188 K, a second-order crystallographic transformation from orthorhombic Pbnm to monoclinic Pb11 , which is accompanied by G-type orbital ordering (OO), takes place.^{16,17} With decreasing temperature, the HoVO_3 compound presents a Néel transition at $T \sim 110$ K due to the occurrence of antiferromagnetic C-type order of the vanadium sublattice.¹⁶ A first-order structural phase transition from the monoclinic to the low-temperature orthorhombic symmetry occurs at $T \sim 40$ K. This transition is characterized by the rearrangement of orbitals into a C-type order and the change of the vanadium magnetic moments to a G-type order.¹⁶ In this paper, we mainly investigate the magnetocaloric properties of HoVO_3 single crystals. We demonstrate that the refrigerant capacity of HoVO_3 vanadate exceeds largely that exhibited by any known RMnO_3 manganite.

II. EXPERIMENTAL

The HoVO_3 single crystals were grown by the travelling floating zone (TFZ) method using polycrystalline samples as described in Ref. 19. Initially, powder of HoVO_4 was prepared by solid state reaction at high temperature using Ho_2O_3 and V_2O_5 as starting elements. The polycrystalline HoVO_3 used for the TFZ growth was then obtained by annealing the HoVO_4 powder in a flow of pure gas of H_2 at 1000°C . The quality of the crystal and its composition were systematically checked by Laue XRD and electron probe microanalysis. Raman spectra as a function of temperature were carried out with the help of a Labram-800 micro-Raman spectrometer equipped with a He-Ne laser and a nitrogen-cooled charge coupled device detector (CCD). Magnetization measurements were realized using a commercial superconducting quantum interference device (SQUID) from Quantum Design, model MPMS XL.

^{a)}E-mail: Mohamed.balli@Usherbrooke.ca.

III. RESULTS AND DISCUSSION

The measured magnetization curves along the crystal axes show that the magnetocrystalline anisotropy between the b and c axes is rather low in HoVO_3 (Fig. 1(a)). Thus, the measurements reported here were mainly carried out along b-axis with the largest magnetization. Figure 1(b) shows the zero-field-cooled and field-cooled magnetization as a function of temperature measured in an external magnetic field of 0.1 T along the b-axis. Taking into account the derivative (dM/dT) of the ZFC thermomagnetic curve shown in the inset of Fig. 1(b), one observes distinguished features at ~ 4 K, ~ 15 K, and ~ 40 K. The observed peak at T_{Ho} (15 K) can be ascribed to the ferromagnetic (FM) ordering of the Ho magnetic moments, while the anomaly at T_1 (4 K) corresponds to the onset of an antiferromagnetic (AF) order of the holmium moments, which is consistent with previous works.^{16–18} The observed small peak at $T_S = 40$ K in the dM/dT curve (inset of Fig. 1(b)) can be attributed to the structural transition from the monoclinic Pb11 symmetry to the low temperature orthorhombic phase. This involves a change in the type of orbitals ordering in HoVO_3 , combined with a spin reorientation of the V^{3+} sublattice.^{16–18}

It is worth noting that the magnetic structure of HoVO_3 for temperatures below 40 K is not well understood and only few studies covering this temperature range were reported.^{16–18}

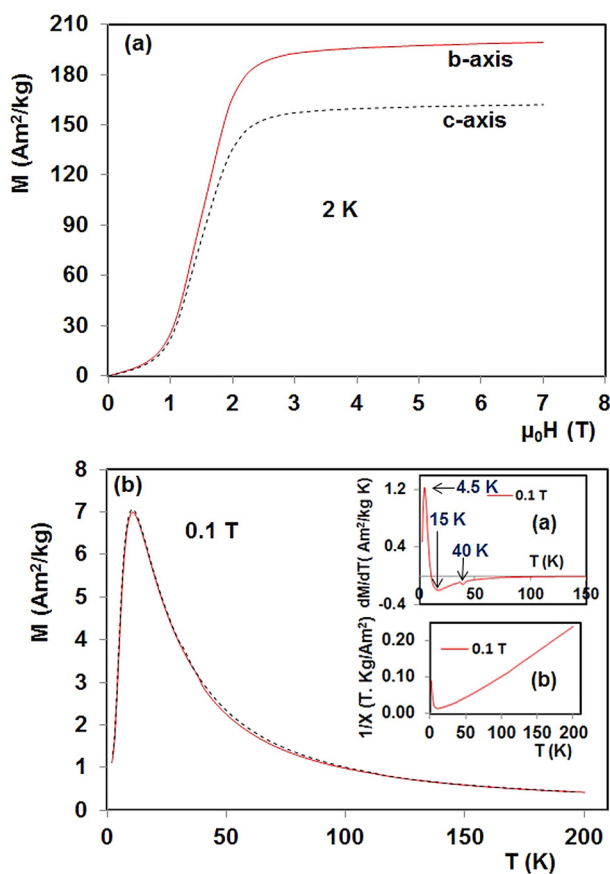


FIG. 1. (a) Isothermal magnetization curves of HoVO_3 single crystal for the b and c axes at 2 K. (b) Temperature dependence of ZFC (continuous line) and FC (dotted line) magnetization of HoVO_3 under a magnetic field of 0.1 T along the axis b. Inset: 0.1 T – dM/dT (a) and ZFC reciprocal susceptibility (b) as a function of temperature.

Blake *et al.*¹⁷ have shown by polarized neutron diffraction that the Ho^{3+} spins have a rather strong ferromagnetic component along the a-axis and an antiferromagnetic component in the b-direction at $T \sim 10$ K. Fujioka *et al.*¹⁸ have observed two pronounced anomalies at 36 K and 11 K in the magnetization and the dielectric constant measurements. They attributed the 11 K feature to the phase transition between the C-type spins ordering (SO)/G-type orbital ordering (high-temperature phase) to the G-type SO/C-type OO (low-temperature phase), while the origin of the critical point at 37 K is not known. On the other hand, Reehuis *et al.*¹⁶ have shown with the help of neutron diffraction that the structural phase transformation (orthorhombic-monoclinic) and the reorientation of the vanadium magnetic moments in the temperature range between 23.5 K and 35 K are strongly coupled to the Ho^{3+} magnetic moments.

As shown in Fig. 1(b), additional critical points resulting from the magnetic transitions of the vanadium sublattice are not visible in the thermomagnetic curves.^{16–18} This can be mainly attributed to the large magnetization of the holmium sublattice (Ho^{3+}), which overshadows the anomalies involving the much smaller magnetization of the vanadium (V^{3+}). Inset of Fig. 1(b) shows the ZFC reciprocal magnetic susceptibility ($1/\chi$) as a function of temperature measured in a field of 0.1 T. The reciprocal susceptibility of HoVO_3 for high temperatures reveals a linear regime, following the Curie-Weiss law. From the linear fit of $1/\chi$, the effective magnetic moment is evaluated to be $11\mu_B$, which is close to the theoretically expected value

$$\text{given by } \mu_{\text{eff}} = \sqrt{(\mu_{\text{eff}}(\text{Ho}^{3+}))^2 + (\mu_{\text{eff}}(\text{V}^{3+}))^2} = 12.28\mu_B.$$

On the other hand, the antiferromagnetic ordering in HoVO_3 under low magnetic fields can be observed in the M-H curves as reported in Fig. 1(a). The magnetization at 2 K is found to increase linearly at low fields followed by a rapid increase to reach the saturation state after overpassing a critical magnetic field. This transition is a typical behaviour of materials exhibiting AF-FM transitions.²⁰ From Fig. 2(a), the AF order occurs under low magnetic fields, whereas the FM order takes place above 1.5 T. However, neutron diffraction measurements are needed to confirm this fact. For HoVO_3 , the saturation of the magnetization could be attributed to the FM ordering of the Ho^{3+} magnetic moments under application of an external magnetic field. The obtained magnetic moment at 2 K for fields higher than 3 T applied along the b-direction is about $200 \text{ Am}^2/\text{kg}$ ($9.45\mu_B$), which is similar to the total magnetic moment of holmium ions ($9.4\mu_B$) determined at liquid helium temperature (4.2 K) by Bombik *et al.*²¹ using neutron diffraction. Considering the fact that the contribution of the V^{3+} moments is negligible,²¹ this result suggests that the Ho^{3+} moments in HoVO_3 can be completely aligned by using sufficiently high magnetic fields, leading to a large magnetization.

The magnetocaloric effect, which can be represented by the isothermal entropy change, was determined from magnetization isotherms shown in Fig. 2(b) by integrating the well-known Maxwell relation.^{22,23} Figure 3(a) displays the entropy change as a function of temperature under several magnetic field variations up to 7 T. As shown, ΔS (T) profiles reveal two pronounced maxima centred at $T_1 \sim 4$ K, and $T_{\text{Ho}} \sim 15$ K, corresponding to the transition temperatures

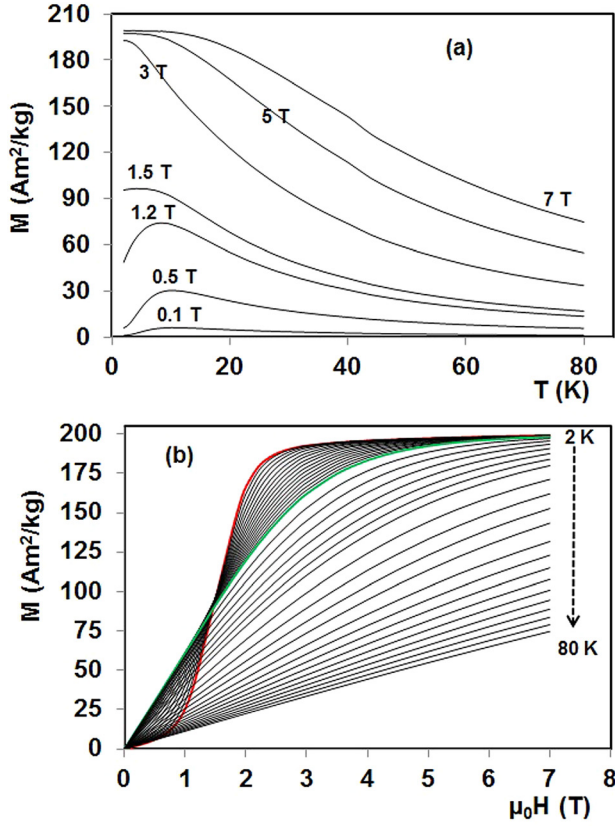


FIG. 2. (a) Magnetization of HoVO₃ single crystal as a function of temperature for different magnetic fields (along the b-axis). (b) Magnetization isotherms of HoVO₃ single crystal in the temperature range 2–80 K with different steps (along the b-axis). The increments of temperature are 0.5 K for 2–10 K, 2 K for 10–24 K, and 4 K for 24–80 K. Isothermal magnetization curves were also collected (not shown here) with increasing and decreasing magnetic field around the ordering temperatures of HoVO₃, showing a very small and negligible hysteresis.

detected in the thermomagnetic curves (inset of Fig. 1(b)). For low magnetic fields, a large negative (or inverse) magnetocaloric effect, which manifests itself as positive values of ΔS , is observed around 4 K, revealing that the HoVO₃ vanadate can be cooled down under the effect of an increasing external magnetic field. This can be attributed to the growing disorder of the antiferromagnetic phase under the application of an external magnetic field along the b-axis. On the other hand, looking at Maxwell relation,^{22,23} the sign and the nature of the MCE (inverse or conventional) are governed by the sign of (dM/dT) . As demonstrated in Fig. 2(a), dM/dT around 4 K is positive for low fields (≤ 1.5 T) giving rise to a negative MCE. For a magnetic field variation of 1.4 T, the maximum change of ΔS is 7.7 J/kg K. The observed large negative MCE could be attributed mainly to the first order character of the transition (AF order-to-FM order) from the low magnetization state to the high magnetization phase occurring around 4 K. Usually, an order-to-order magnetic transition is of first order in nature. However, the nature of the magnetic phase transition was also confirmed from the Arrott plots (H/M vs M^2),²⁴ which exhibit a negative slope around 4 K (Fig. 3(b)). According to Banerjee criterion,²⁴ a negative or positive slope of H/M versus M^2 indicates a first-order or second-order transition, respectively.

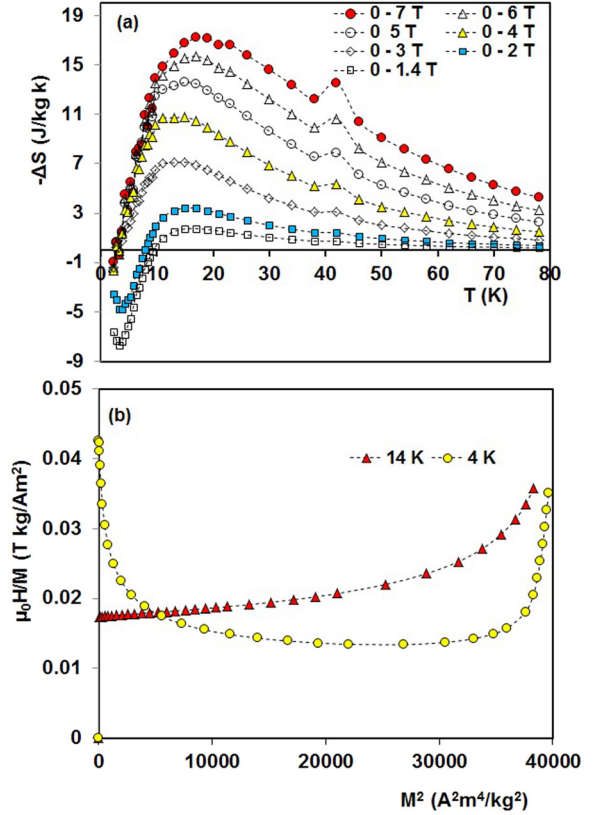


FIG. 3. (a) Isothermal entropy change of HoVO₃ single crystal as a function of temperature for several magnetic fields (along the b-axis). (b) Arrott plots close to the magnetic phase transitions taking place at T_i and T_{Ho} .

As shown in Figure 3(a), this negative MCE disappears for sufficiently high magnetic fields, which is due to the “ferromagnetic” ordered state of the Ho³⁺ moments becoming dominant with increasing external magnetic field. In addition to the inverse MCE, the HoVO₃ single crystal shows a giant MCE in the vicinity of the second order magnetic phase transition (positive slope of Arrott plots, Fig. 3(b)) from the “ferromagnetic” to the “paramagnetic” state around $T_{Ho} = 15$ K. For a magnetic field change of 5 T and 7 T, the maximum entropy change is found to be about 13.6 J/kg K and 17.2 J/kg K, respectively. These values are comparable to the isothermal entropy change reported for RMnO₃ manganites ($R = \text{Tb, Ho, Dy}$)^{11,14,15} and much larger, in comparison with TmMnO₃.²⁵

It is worth noting that the RVO₃ vanadates reveal a weak specific heat at low temperatures (around 10 K).^{26–28} Consequently, a large adiabatic temperature change is expected in HoVO₃. According to Refs. 26–28, the RVO₃ specific heat is evaluated to be ~ 3.4 J/mole K in the temperature range around 10 K. Based on this value, the maximum adiabatic temperature change exhibited by HoVO₃ [estimated from $\Delta T_{ad} = -(T/C_p) \Delta S$ (Ref. 29)] was found to show a gigantic value as large as 15.5 and 23.5 K under 5 and 7 T, respectively. The maximum ΔT_{ad} revealed by HoVO₃ is much larger than that presented by the Dy_{0.25}Er_{0.75}Al₂ intermetallic, which is considered as a promising magnetic refrigerant in a similar temperature range.²⁹ Under 7.5 T, only a maximum temperature change of 11 K was

reported in $\text{Dy}_{0.25}\text{Er}_{0.75}\text{Al}_2$.²⁹ However, to better evaluate the adiabatic temperature changes of the here studied material, heat capacity measurements under several magnetic fields must be performed to determine the full entropy curves and accordingly, ΔT_{ad} . This will be the subject of a future investigation.

On the other hand, $-\Delta S(T)$ curves reveal a third peak around 40 K, enlarging consequently the working temperature range of HoVO_3 . In contrast with the HoVO_3 vanadate, such peak has not been observed in the RMnO_3 manganites.^{14,15,25} As discussed above, the peak at $T_S \sim 40$ K is attributed to the magnetostructural transition coupled with a rearrangement of the V^{3+} sublattice orbitals.^{16–18} In order to gain more insight on the origin of this peak, a Raman scattering investigation was performed. In Fig. 4, we report in the temperature range close to T_S the Raman active excitations of HoVO_3 with the incident light perpendicular to the bc plane. The phonons are compared with the YMnO_3 modes reported in Ref. 30, and their symmetries are assigned using an analyzer. At ~ 40 K, the $\text{Ag}(\text{O})$ phonon mode is observed at 330 cm^{-1} , while the alpha excitation appears around 370 cm^{-1} . This latter excitation has an electronic origin and appears when the G-OO/C-SO phase is established.³¹ Below 40 K, two new excitations, which are associated with the structural, magnetic, and orbital transitions, appear at 340 cm^{-1} (Ag(O) phonon in the C-OO/G-SO phase) and 400 cm^{-1} (β excitation identified either as orbiton or magnon^{31–33}). The Raman shift jump of 10 cm^{-1} of the Ag(O) phonon in the transition G-OO/C-SO phase to the C-OO/G-SO phase denotes the presence of the first order structural transition.

From a practical point of view, the refrigerant capacity (RC) is an important figure of merit for the evaluation of magnetocaloric materials in the aim of their implementation in working devices. The RC measures the transferred energy between hot and cold sources and involves both, the MCE magnitude and the working temperature range. It is given by $RC = \int_{T_C}^{T_H} \Delta S(T) dT$ which is equivalent to the area under the ΔS versus T plot with T_C and T_H , being the temperatures at half maximum of the $-\Delta S(T)$ peak, and taken as the

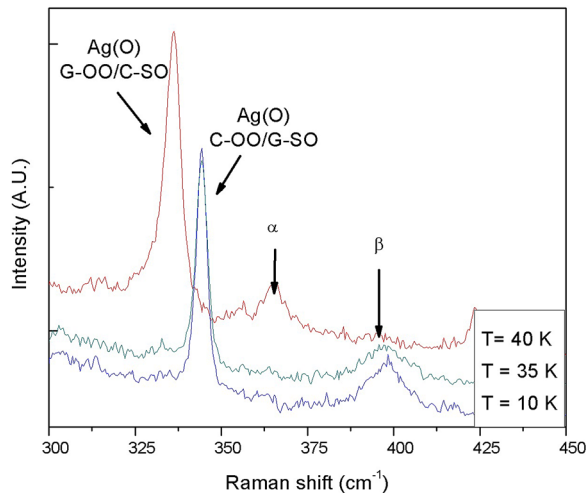


FIG. 4. Micro-Raman spectra at 10 K, 35 K, and 40 K for HoVO_3 single crystal.

integration limits. Calculations reveal that the single crystal HoVO_3 exhibits a giant refrigerant capacity. For magnetic field variations of 5 T and 7 T, RC values reach 400 J/kg and 620 J/kg, respectively, which exceed largely the RC of any known RMnO_3 manganite^{10,14,15,25} reported in similar temperature range (see Fig. 5(a)). The relative cooling power (RCP), which is the product of the maximum isothermal entropy change and full width at half maximum (FWHM) [$RCP = -\Delta S_{\text{max}} * \Delta T_{\text{FWHM}}$], is found to be 534 J/kg and 800 J/kg for 5 T and 7 T, respectively. One should notice that the RC exhibited by the HoMnO_3 manganite is only 382 J/kg under 7 T, which means that the RC can be markedly improved (by more than 62%) with the vanadate.

The enhancement of the refrigerant capacity in the HoVO_3 vanadate in comparison with the RMnO_3 manganites can be attributed to different factors. First, the Ho^{3+} magnetic moments in HoVO_3 can be completely aligned giving rise to a large magnetization, and, consequently, a large ΔS . Second, the $-\Delta S$ peaks corresponding to the magnetic ordering of the Ho^{3+} moments around 15 K and the structural transition around 40 K partly overlap leading to a wide working temperature range. Finally, in contrast to the RMnO_3 manganites, the Ho^{3+} magnetic moments in HoVO_3 remain meaningfully polarized¹⁸ even at temperatures far above T_{Ho} (inset Fig. 5(b)), which also contributes to the broadening of the $-\Delta S(T)$ curve (Fig. 5(b)), enhancing consequently the refrigerant capacity. As reported in Fig. 5(b), the $-\Delta S(T)$

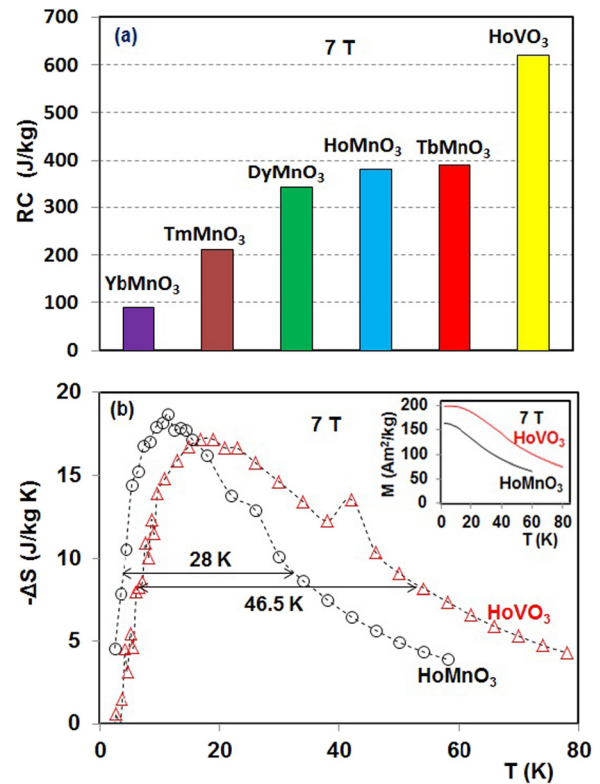


FIG. 5. (a) Refrigerant capacity of the HoVO_3 vanadate under 7 T (along the b-axis). RC for different RMnO_3 manganites with $R = \text{Yb}$ (Ref. 14), Tm (Ref. 25), Dy (Ref. 15), Ho (own sample), and Tb (Ref. 10) are also shown for comparison. (b) Isothermal entropy changes of HoVO_3 and HoMnO_3 single crystals as a function of temperature under 7 T. Inset: Thermomagnetic curves of HoVO_3 and HoMnO_3 single crystals under 7 T.

FWHM exhibited by HoVO_3 under 7 T is about 46.5 K, while it is only 28 K for HoMnO_3 . According to recent reports, the V^{3+} sub-lattice could play an important role in the magnetic polarization of the Ho^{3+} moments at high temperatures.^{16,18} As a comparison, the magnetic and magnetocaloric properties of the HoMnO_3 single crystal (own sample) are shown in Fig. 5. The RC values exhibited by HoVO_3 are also comparable or much higher than some of the best intermetallic materials with similar working temperature range such as HoPdIn (476 J/kg for 7 T),³⁴ ErMn_2Si_2 (273 J/kg for 5 T),³⁵ ErRuSi (312 J/kg for 5 T),³⁶ DySb (144 J/kg for 5 T),³⁷ TmGa (364 J/kg for 5 T),³⁸ TmCuAl (371 J/kg for 5 T),³⁹ EuSe (435 J/kg for 5 T),⁴⁰ and TbGa (900 J/kg for 7 T).⁴¹ However, when compared with intermetallic refrigerants, HoVO_3 exhibits a high resistance against corrosion and oxidation, which is highly required in applications. In addition, HoVO_3 is a Mott insulator at low temperatures,^{16–18} which prevents energy losses caused by eddy currents when varying the magnetic field in a functional device.

IV. CONCLUSIONS

In summary, HoVO_3 single crystal magnetic and magnetocaloric properties are studied. They reveal a series of magnetic phase transitions yielding to a negative and conventional magnetocaloric effects. At low temperatures (<50 K), three phase transitions are observed. A first order transition from antiferromagnetic to ferromagnetic state occurs at $T_i \sim 4$ K, followed by a second order transition at $T_{\text{Ho}} \sim 15$ K due to the disorder of the ferromagnetic phase. Finally, a structural transformation from the monoclinic to the low temperature orthorhombic symmetry takes place at $T_S \sim 40$ K. Under low magnetic fields, a large negative MCE ($\Delta S = 7.7$ J/kg K for 1.4 T), which originates from the antiferromagnetic phase, can be obtained around T_i . Additionally, the HoVO_3 compound shows a giant conventional MCE ($\Delta S = -17.2$ J/kg K for 7 T) without thermal and magnetic hysteresis close to T_{Ho} . Under a magnetic field change of 7 T, the estimated adiabatic temperature change is found to be larger than 23.5 K. On the other hand, the obtained RC (620 J/kg for 7 T) is much larger than any known RMnO_3 type-manganite and even larger than some of the best intermetallic materials with similar working temperature range. The present results combined with the high electrical resistance and the chemical stability render the HoVO_3 vanadate as a promising refrigerant for application at low temperature regime. Our results provide also new avenues for the enhancement of the magnetothermal capacity in ABO_3 oxides.

ACKNOWLEDGMENTS

The authors thank M. Castonguay and S. Pelletier for technical support. We acknowledge the financial support from NSERC (Canada), FQRNT (Québec), CFI, CIFAR, and the Université de Sherbrooke.

¹K. A. Gschneidner, Jr., V. K. Pecharsky, and A. O. Tsokol, *Rep. Prog. Phys.* **68**, 1479 (2005).

²V. K. Pecharsky and K. A. Gschneidner, Jr., *Phys. Rev. Lett.* **78**, 4494 (1997).

³H. Wada and Y. Tanabe, *Appl. Phys. Lett.* **79**, 3302 (2001).

- ⁴O. Tegus, E. Brück, K. H. J. Buschow, and F. R. de Boer, *Nature* **415**, 150 (2002).
- ⁵A. Fujita, S. Fujieda, Y. Hasegawa, and K. Fukamichi, *Phys. Rev. B* **67**, 104416 (2003).
- ⁶F. X. Hu, B. G. Shen, J. R. Sun, G. J. Wang, and Z. H. Cheng, *Appl. Phys. Lett.* **80**, 826 (2002).
- ⁷M. Balli, D. Fruchart, and D. Gignoux, *Appl. Phys. Lett.* **92**, 232505 (2008).
- ⁸M. H. Phan and S. C. Yu, *J. Magn. Magn. Mater.* **308**, 325 (2007).
- ⁹M. Balli, S. Jandl, P. Fournier, and M. M. Gospodinov, *Appl. Phys. Lett.* **104**, 232402 (2014).
- ¹⁰J.-L. Jin, X.-Q. Zhang, G.-K. Li, Z.-H. Cheng, L. Zheng, and Y. Lu, *Phys. Rev. B* **83**, 184431 (2011).
- ¹¹C. R. H. Bahl, D. Velazquez, K. K. Nielsen, K. Engelbrecht, K. B. Andersen, R. Bulatova, and N. Pryds, *Appl. Phys. Lett.* **100**, 121905 (2012).
- ¹²T. Kimura, T. Goto, H. Shintani, K. Ishizaka, T. Arima, and Y. Tokura, *Nature* **426**, 55 (2003).
- ¹³T. Lottermoser, T. Lonkai, U. Amann, D. Hohlwein, J. Ihringer, and M. Fiebig, *Nature* **430**, 541 (2004).
- ¹⁴A. Midya, S. N. Das, P. Mandal, S. Pandya, and V. Ganesan, *Phys. Rev. B* **84**, 235127 (2011).
- ¹⁵M. Balli, S. Jandl, P. Fournier, S. Mansouri, A. Mukhin, Yu. V. Ivanov, and A. M. Balbashov, *J. Magn. Magn. Mater.* **374**, 252 (2015).
- ¹⁶M. Reehuis, C. Ulrich, K. Prokes, S. Mat'as, J. Fujioka, S. Miyasaka, Y. Tokura, and B. Keimer, *Phys. Rev. B* **83**, 064404 (2011).
- ¹⁷G. R. Blake, A. A. Nugroho, M. J. Gutmann, and T. T. M. Palstra, *Phys. Rev. B* **79**, 045101 (2009).
- ¹⁸J. Fujioka, T. Yasue, S. Miyasaka, Y. Yamasaki, T. Arima, H. Sagayama, T. Inami, K. Ishii, and Y. Tokura, *Phys. Rev. B* **82**, 144425 (2010).
- ¹⁹G. R. Blake, T. T. M. Palstra, Y. Ren, A. A. Nugroho, and A. A. Menovsky, *Phys. Rev. B* **65**, 174112 (2002).
- ²⁰M. Balli, D. Fruchart, and R. Zach, *J. Appl. Phys.* **115**, 203909 (2014).
- ²¹A. Bombik, B. Lesniewska, and A. Oles, *Phys. Status Solidi A* **50**, K17 (1978).
- ²²G. J. Liu, J. R. Sun, J. Shen, B. Gao, H. W. Zhang, F. X. Hu, and B. G. Shen, *Appl. Phys. Lett.* **90**, 032507 (2007).
- ²³M. Balli, D. Fruchart, D. Gignoux, and R. Zach, *Appl. Phys. Lett.* **95**, 072509 (2009).
- ²⁴B. K. Banerjee, *Phys. Lett.* **12**, 16 (1964).
- ²⁵J.-L. Jin, X.-Q. Zhang, H. Ge, and Z.-H. Cheng, *Phys. Rev. B* **85**, 214426 (2012).
- ²⁶J.-Q. Yan, H. B. Cao, M. A. McGuire, Y. Ren, B. C. Sales, and D. G. Mandrus, *Phys. Rev. B* **87**, 224404 (2013).
- ²⁷B. Zhao, Y. Huang, J. Yang, D. Dai, J. Dai, and Y. Sun, *J. Alloys Compds.* **558**, 222 (2013).
- ²⁸S. Miyasaka, Y. Okimoto, M. Iwama, and Y. Tokura, *Phys. Rev. B* **68**, 100406 (R) (2003).
- ²⁹A. M. Tishin and Y. I. Spichkin, *The Magnetocaloric Effect and Its Applications* (IOP Publishing Ltd, London, 2003).
- ³⁰M. N. Iliev, M. V. Abrashev, H. G. Lee, V. N. Popov, Y. Y. Sun, C. Thomsen, T. L. Meng, and C. W. Chu, *J. Phys. Chem. Solids* **59**, 1982 (1998).
- ³¹S. Sugai and K. Hirota, *Phys. Rev. B* **73**, 020409 (2006).
- ³²S. Miyasaka, J. Fujioka, M. Iwama, Y. Okimoto, and Y. Tokura, *Phys. Rev. B* **73**, 224436 (2006).
- ³³J. Reul, A. A. Nugroho, T. T. M. Palstra, and M. Gruninger, *Phys. Rev. B* **86**, 125128 (2012).
- ³⁴L. Li, T. Namiki, D. Huo, Z. Qian, and K. Nishimura, *Appl. Phys. Lett.* **103**, 222405 (2013).
- ³⁵L. Li, K. Nishimura, W. D. Hutchison, Z. Qian, D. Huo, and T. NamiKi, *Appl. Phys. Lett.* **100**, 152403 (2012).
- ³⁶S. B. Gupta and K. G. Suresh, *Appl. Phys. Lett.* **102**, 022408 (2013).
- ³⁷W. J. Hu, J. Du, B. Li, Q. Zhang, and Z. D. Zhang, *Appl. Phys. Lett.* **92**, 192505 (2008).
- ³⁸Z. J. Mo, J. Shen, L. Q. Yan, C. C. Tang, J. Lin, J. F. Wu, J. R. Sun, L. C. Wang, X. Q. Zheng, and B. G. Shen, *Appl. Phys. Lett.* **103**, 052409 (2013).
- ³⁹Z. J. Mo, J. Shen, L. Q. Yan, J. F. Wu, and L. C. Shen, *Appl. Phys. Lett.* **102**, 192407 (2013).
- ⁴⁰D. X. Li, T. Yamamura, S. Nimori, Y. Homma, F. Honda, and D. Aoki, *Appl. Phys. Lett.* **102**, 152409 (2013).
- ⁴¹X. Q. Zheng, J. Chen, J. Shen, H. Zhang, Z. Y. Xu, W. W. Gao, J. F. Wu, F. X. Hu, J. R. Sun, and B. G. Shen, *J. Appl. Phys.* **111**, 07A917 (2012).